Biosensors and Bioelectronics 143 (2019) 111618

Contents lists available at ScienceDirect

Biosensors and Bioelectronics

journal homepage: www.elsevier.com/locate/bios

Dependent signal quenching and enhancing triggered by bipedal DNA walker for ultrasensitive photoelectrochemical biosensor

Minghui Zhu, Xia Zhong, Hanmei Deng, Liaojing Huang, Ruo Yuan*, Yali Yuan**

Education Ministry Key Laboratory on Luminescence and Real-Time Analysis, College of Chemistry and Chemical Engineering, Southwest University, Chongqing, 400715, People's Republic of China

ARTICLE INFO

Keywords:
Photoelectrochemical biosensor
Bipedal DNA walker
On-off-super on
Thrombin

ABSTRACT

Herein, by utilizing bipedal DNA walker as booster to adjust the distance of quencher ferrocene (Fc) and sensitizer methylene blue (MB) to photoactive material perylene-3,4,9,10-tetracarboxylic acid (PTCA), a novel "on-off-super on" photoelectrochemical (PEC) biosensor was proposed for ultrasensitive detection of thrombin (TB). Firstly, the PTCA matrix on electrode could provide a high initial PEC signal assisted by depAu. Upon the Fc labeled on hairpin DNA 1 (H_1-Fc) proximate to PTCA, the PEC signal could obviously decrease to reduce the background signal. Interestingly, the target TB-related bipedal DNA walker implemented the opening of H_1-Fc for the departure of Fc toward PTCA, which achieved the recovery of PEC signal and exposed the prelocked toehold domain for the hybridization with hairpin DNA 2 labeled with MB (H_2-MB), thereby making the MB approach to PTCA for achieving the "super on" signal. As a result, this proposed strategy showed a wide linear range from 0.5 fM to 100 nM with a low detection limit down to 0.17 fM for TB detection, providing an efficient and available avenue for sensitive detection of biomolecules in bioanalysis and disease diagnosis.

1. Introduction

Photoelectrochemical (PEC) assay, as a newly emerging and promising analytical technique, has aroused widespread interest of researchers with the desirable merits of simple equipment, low background signal, high sensitivity and excellent stability (Chu et al., 2019; Gill et al., 2008; Lee et al., 2018; Liu et al., 2018; Zhao et al., 2014, 2015). To date, many PEC-based biosensors have been reported to analyze various targets, such as proteins (Mei et al., 2018; Zhang et al., 2018a), nucleic acid sequences (Hou et al., 2015; Li et al., 2015; Zhang et al., 2018b), cells (Li et al., 2017b, 2018a; Wang et al., 2016) and biomarkers (Liu et al., 2016; Zeng et al., 2019a, 2019b). Nevertheless, most of them were fabricated in "signal on" (Wang et al., 2018a; Yan et al., 2018; Yu et al., 2019) or "signal off" (Qileng et al., 2018; Wang et al., 2018b; Yan et al., 2015) modes with photoactive material previously assembled on electrode, thereby leading to the non-negligible background for restraining the improvement of detection accuracy and sensitivity despite the cooperation of multiple sensitizers or quenchers. Accordingly, our group (Li et al., 2016) and Yu's group (Kong et al., 2018) thereafter constructed the "on-off-on" PEC modes, in which the first "on" state with high initial PEC signal offered a precondition for sensitive detection while the "off" state with low PEC signal reduced the background signal. However, the enhancement of second "on" signal reported at present was mainly derived from the departure of quenchers that enabling only up to 100% signal recovery, which thus became the bottleneck for further improving the detection range and sensitivity of PEC biosensor.

To overcome this issue, we proposed a novel "on-off-super on" mode based on distance-controllable signal quenching and enhancing, in which both the departure of quencher and approach of sensitizer realized by the bipedal DNA walker would cooperate on the enhancement of the second "on" signal for achieving "super on" state, making the detection range and sensitivity improved effectively. To make this proposal into a reality, choosing the suitable quencher and sensitizer for cooperating on photoactive material under the same irradiated wavelength would be the important key and still a challenge. Coincidentally, we discovered that the small molecules methylene blue (MB) and ferrocene (Fc) showed outstanding sensitizing and quenching effect to the photoactive material perylene-3,4,9,10-tetracarboxylic acid (PTCA), respectively, which enabled them to be assembled on signal-DNA strands for implementing the distance-controllable signal quenching and enhancing effect via DNA regulator.

Based on the observation mentioned above, herein, by utilizing the bipedal DNA walker that composed with target thrombin (TB) and two

* Corresponding author.
** Corresponding author.
E-mail addresses: yuanruo@swu.edu.cn (R. Yuan), y198688@swu.edu.cn (Y. Yuan).

https://doi.org/10.1016/j.bios.2019.111618
Received 12 August 2019; Accepted 19 August 2019
Available online 22 August 2019
0956-5663/

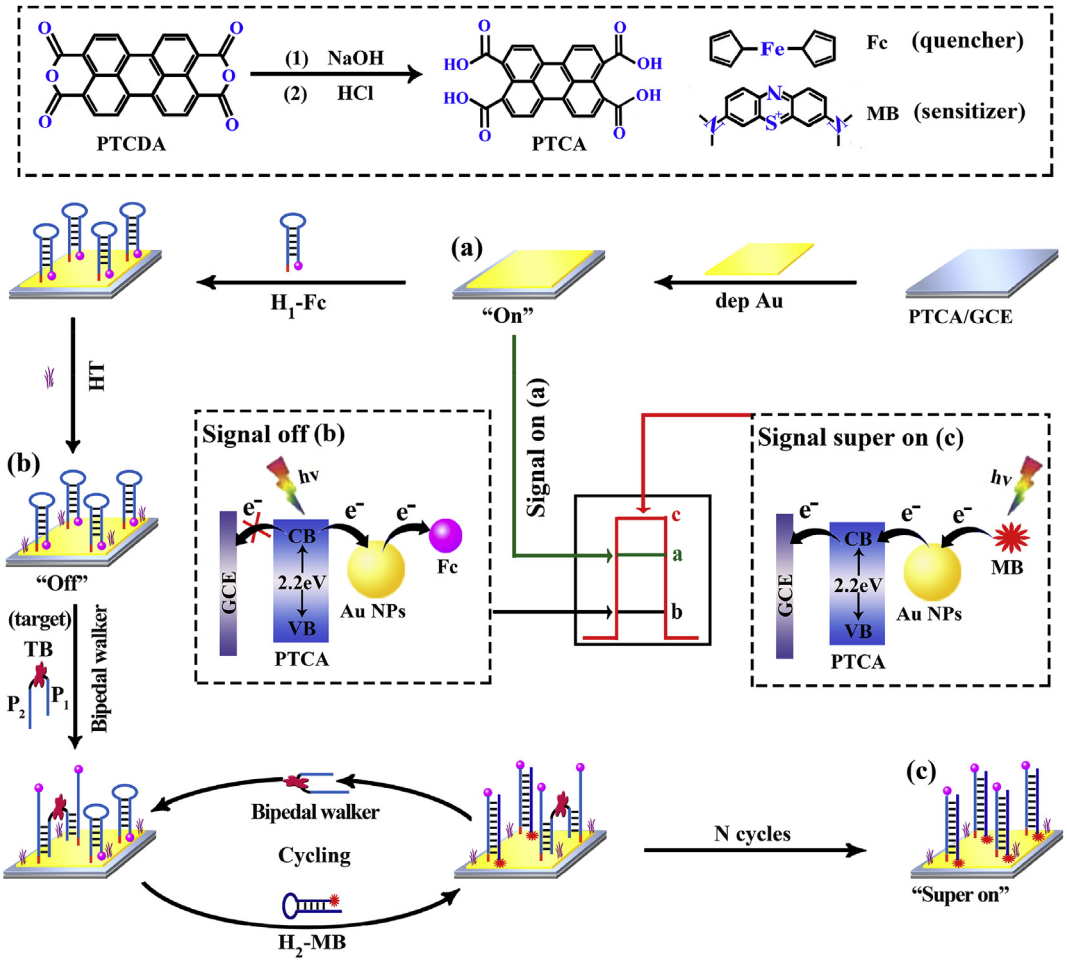

Scheme 1. Schematic of "On-Off-Super on" Strategy of TB Detection by Using Bipedal DNA Walker to Adjust the Distance of Quencher and Sensitizer for Controlling the PEC Signals.

aptamers (P_1 and P_2) as a regulator to adjust the distance of Fc and MB toward PTCA for controlling the signal quenching and enhancing, we fabricated a novel "on-off-super on" PEC biosensor for ultrasensitive detection of TB. As shown in Scheme 1, the initially desirable "signal on" state was obtained by electrodepositing conductive depAu onto abundant PTCA decorated electrode. After further self-assembling of Fc labeled hairpin DNA 1 (H_1-Fc) via Au–S bond, an obvious "signal off" state was thus appeared owing to the valid quenching effect caused by proximate distance between Fc and PTCA, which obviously reduced the background signal. Afterwards, the TB-related bipedal DNA walker was used to open the hairpin H_1-Fc for enlarging the distance between Fc and PTCA, which achieved the recovery of PEC signal. Meanwhile, the added hairpin DNA 2 labeled with MB (H_2-MB) could hybridized with opened H_1-Fc to make the sensitizer MB close enough to PTCA and release the bipedal DNA walker for next recycling, thereby further enhancing the PEC signal to obtain "super on" signal. Such an "on-off-super on" strategy not only inherited the merits of low background signal from "on-off-on" mode, but also significantly enhanced the second "on" signal with improved detection range and sensitivity. Furthermore, the proposed PEC strategy based on distance-controllable signal quenching and enhancing provided a promising avenue for the ultrasensitive analysis of biomolecules in bioanalysis and disease diagnosis.

2. Experiment

2.1. Fabrication of PEC biosensor

Photoactive material PTCA was synthesized according to the previous reported literature (Lei et al., 2018). Prior to modification, we used 0.3 μm alumina slurry to polish the glass carbon electrode (GCE, 4 mm in diameter) for obtaining mirror surface, followed by using anhydrous ethanol and distillation to ultrasound washing three times, respectively. Then 5.0 μL prepared PTCA was dipped onto the surface of electrode and dried at 37 °C to get thin films. Subsequently, the modified electrode was immersed in 1% $HAuCl_4$ to deposit Au onto the electrode surface with deposition time of 15 s (electrodeposition potential of reference electrode $Hg/HgCl_2$ was −0.2 V). Before H_1-Fc immobilizing onto the depAu/PTCA/GCE surface, the 1.0 μM H_1-Fc was heated to 95 °C for 5 min and slowly cooled down to 25 °C. Then 10 μL 1.0 μM H_1-Fc was dropped onto the surface of depAu/PTCA/GCE for incubating 12 h at 4 °C. Afterwards, adding 5 μL 1.0 mM HT onto the modified electrode surface to incubate 30 min at room temperature for eliminating the nonspecific adsorption sites of sensing interface. Ultimately, 10 μL prepared mixture solution containing 1.2 μM H_2-MB, 150 nM P_2, 150 nM P_1 and various concentrations of TB was incubated for 30 min and then dropped onto the modified electrode to incubate for 80 min at room temperature.

2.2. PEC measurement

The PEC determination was executed in 4 mL PBS (pH = 7.0)

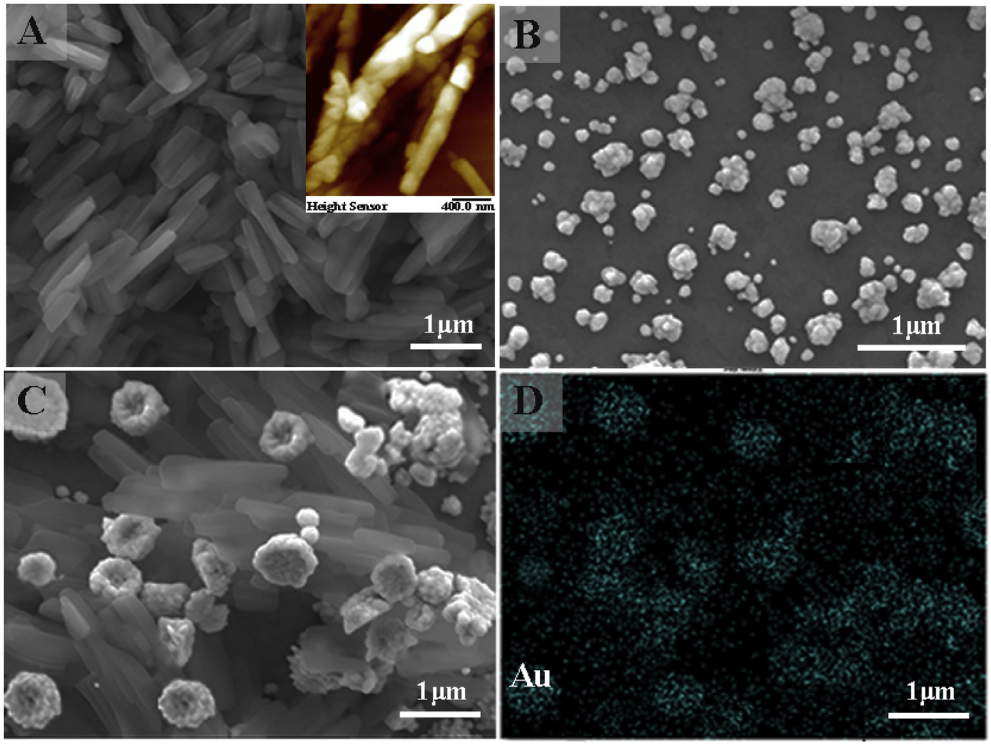

Fig. 1. SEM images of (A) PTCA, (B)depAu, (C)depAu/PTCA and (D) the mapping of Au.

containing 0.01 g electron donor AA. The LED lamp at 460 nm was served as excitation light source to record the PEC signal according to switch off-on-off for 10-20-10 s under 0.0 V potential (*vs* saturated Hg/$HgCl_2$).

3. Discussion

3.1. Characterization of the different nanomaterials

The scanning electron microscopy (SEM) and atomic force microscopy (AFM) were employed to characterize the size and morphology of the prepared nanomaterials. As shown in Fig. 1A, the PTCA displayed the short and rod-like structure with lengths of about 1.0 μm and diameters of around 250 nm resulting from π-π stacking, which was according with previous reports (Lei et al., 2016). Simultaneously, the AFM was also used to characterize the morphology of PTCA. As shown in the illustration of Fig. 1A, the morphology of PTCA was consistent with the morphology in Fig. 1A. As illustrated in Fig. 1B, the larger area of gold seeds and gold nanoflowers were obtained, which manifested the successful preparation of depAu. As illustrated in Fig. 1C, the depAu were distributed on the surface of PTCA after electrodeposition, which showed that the depAu were successfully modified on the surface of PTCA. Furthermore, the element mapping of Au was also characterized to demonstrate the Au distribution (Fig. 1D).

3.2. Characterization of the hybridization reaction triggered by bipedal DNA walker

The polyacrylamide gel electrophoresis (PAGE) was employed to characterize the hybridization reaction triggered by bipedal DNA walker. As shown in Fig. S1 in the Supplementary material, the bright bands of lane 1, lane 2 and lane 3 represented the hairpin DNA of H_1-Fc, the affinity probes of P_1 and P_2, respectively. A bright band of lane 4 could be seen clearly after the affinity probes P_1 and P_2 specifically recognizing TB, which demonstrated that the bipedal DNA walker with the highest molecular weight was constructed successfully. When the H_1-Fc was added into the bipedal DNA walker, a dual band appeared in lane 5, where the top band represented the hybridization product of H_1-Fc and bipedal DNA walker, the other band represented the remaining bipedal DNA walker. The band of lane 6 represented the hairpin DNA of H_2-MB. After adding the H_2-MB, the lane 7 showed two bands. The top band represented the bipedal DNA walker and the remaining band represented the hybridization product of the H_1-Fc and H_2-MB, indicating that the bipedal DNA walker successfully triggered the hybridization of H_1-Fc and H_2-MB via proximal-dependent hybridization on electrode surface.

3.3. PEC and EIS characterization of biosensor

The step-by-step construction for the PEC biosensor was characterized by PEC measurement. As displayed in Fig. 2A, the PTCA modified electrode showed an obvious photocurrent (curve b) due to its excellent photoelectric conversion efficiency in comparison with the photocurrent of bare electrode (curve a). After modifying with depAu, the electrode also exhibited an enhanced photocurrent (curve c) because the energetic electrons from the surface plasmons of the depAu were injected into the LUMO orbit of the PTCA (Li et al., 2014). The photocurrent decreased significantly after the modification of H_1-Fc (curve d), which may be interpreted that Fc can be treated as the quencher for effectively decreasing the photocurrent of PTCA. Then, the photocurrent continually decreased (curve e) with the successive modification of HT. However, photocurrent increased dramatically after the HT/H_1-Fc/depAu/PTCA/GCE subjecting to the mixture of P_1, P_2, H_2-MB and TB (curve f), which can be attributed to the prominent photoelectric activity of MB, the reduced quenching effect of Fc and low steric hindrance effect caused by the released bipedal DNA walker. These obtained results demonstrated the bipedal DNA walker could trigger the hybridization reaction to adjust the distance of quencher and sensitizer for enhancing PEC signal.

Furthermore, the interface properties of the modified electrode were also studied by the effective technique of electrochemical impedance spectroscopy (EIS) during each step modification. Each impedance

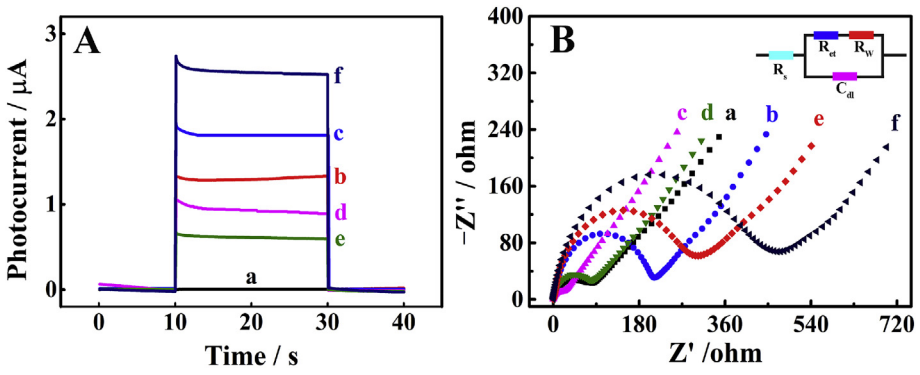

Fig. 2. (A) PEC responses and (B) EIS profiles of (a) bare GCE, (b) PTCA/GCE, (c) depAu/PTCA/GCE, (d) H_1-Fc/depAu/PTCA/GCE, (e) HT/H_1-Fc/depAu/PTCA/GCE, (f) HT/H_1-Fc/depAu/PTCA/GCE treated with mixture of H_2-MB, P_1, P_2 and TB. Photocurrent was measured in 4 mL PBS containing 0.01 g AA at 0.0 V potential (*vs* saturated $Hg/HgCl_2$). EIS was performed in PBS (pH = 7.0) containing 5.0 mM $K_3[Fe(CN)_6]/K_4[Fe(CN)_6]$ and 0.1 M KCl in the frequency range between 0.1 Hz and 100 kHz at the amplitude of 5 mV.

spectra in this strategy was monitored in PBS (pH = 7.0) containing 5.0 mM $K_3[Fe(CN)_6]/K_4[Fe(CN)_6]$(1:1) and 0.1 M KCl. The impedance spectra were shown in Fig. 2B for each step modification of biosensors. The impedance spectrum of the bare electrode (curve a) showed a small semicircle, implying the Ret value was relatively small. After the bare electrode modified with PTCA, the Ret value of the modified electrode increased because the PTCA hindered the electron transfer from the solution of $K_3[Fe(CN)_6]/K_4[Fe(CN)_6]$ to electrode (curve b). Nevertheless, with the modification of Au NPs, the semicircle diameter obviously decreased (curve c), which was ascribed to that the outstanding electron transfer property of Au NPs facilitated the electron transfer. Then, the H_1-Fc was incubated onto the modified electrode surface. Although the Fc facilitated the electron transfer, the Ret value still increased on account of the electronic repulsion between negatively charged DNA and $K_3[Fe(CN)_6]/K_4[Fe(CN)_6]$ with negative charge (curve d). After assembling HT on the H_1-Fc/depAu/PTCA/GCE surface, a remarkable enhanced Ret value was obtained (curve e) due to the inaccessibility created by HT. While the mixture of P_1, P_2, H_2-MB and TB was further incubated onto HT/H_1-Fc/depAu/PTCA/GCE surface, the Ret increased again (curve f), which was mainly ascribed to the steric hindrance effect of TB. Therefore, these results demonstrated the PEC biosensor was constructed successfully.

3.4. Comparison of PEC response for different electrodes

Four kinds of electrode were fabricated to demonstrate the "on", the "off" and the "super on" effect of the proposed strategy. As shown in Fig. 3A, the photocurrent increased about 1.79 μA when depAu were deposited onto PTCA/GCE. After the H_1-Fc was modified onto the surface of depAu/PTCA/GCE, the photocurrent reduced by 1.2 μA due to the efficiently quenching effect of Fc which near the electrode surface (Fig. 3B). Regrettably, the photocurrent increased only 0.04 μA after adding the bipedal DNA walker (Fig. 3C), which can be explained by the steric hindrance of the bipedal DNA walker. However, the photocurrent increased by 1.92 μA when the H_2-MB and the bipedal DNA walker were added together (Fig. 3D), thereby achieving the "super on" state. The reasons could be list as follows: first, the bipedal DNA walker opened the H_1-Fc to make Fc far away from the electrode surface for reducing the quenching effect. Second, the H_2-MB hybridized with H_1-Fc to release the bipedal DNA walker which could continue to trigger the hybridization reaction of the H_1-Fc and the H_2-MB, thereby amount of MB was captured on the electrode surface to enhance the photocurrent. Third, the steric hindrance on electrode was obviously reduced when the bipedal DNA walker was released from electrode.

3.5. Optimization of experiment condition

In order to obtain excellent performance of PEC biosensor, the optimization of some vital experimental parameters was quietly necessary. In general, it takes a certain time for a bipedal DNA walker to open H1-Fc for the hybridization reaction with H_2-MB. Thus, the incubation time of the prepared P_1, P_2, TB and H_2-MB mixture on the HT/H_1-Fc/depAu/PTCA/GCE surface in the range from 20 min to 120 min was optimized. As displayed in Fig. S2A in the Supplementary material, in the presence of 20 nM TB, the PEC signal enhanced with the extension of time in the range from 20 min to 80 min and then leveled off after 80 min, indicating that the reaction time of 80 min was the optimal incubation time. Then, various concentrations of H_2-MB were also investigated. Since the MB is the sensitizer for PTCA, which can significantly affect photocurrent signal due to the excellent photoelectric conversion efficiency. In the presence of 20 nM TB, the variation of photocurrent was subtle after the concentration of H_2-MB reaching 1.2 μM in Fig. S2B in the Supplementary material. Therefore, the 1.2 μM of H_2-MB was selected as the optimum concentration for obtaining high analytical performance of the PEC biosensor. Furthermore, in order to prove the amplified effect of this biosensor, the PEC response in the absence and presence of 20 nM TB also were investigated. Clearly seen in Fig. S2C in Supplementary materials, the PEC signal increased significantly in the presence of TB.

3.6. PEC analysis of biosensor for TB detection

The analytical performance of this PEC biosensor for detecting various concentrations of TB was evaluated after optimizing the experimental conditions. As demonstrated in Fig. 4A, the PEC responses constantly enhanced with the increment of various concentrations of TB (the other parameters kept constant: 1.2 μM H_2-MB, 150 nM P_2 and 150 nM P_1) from 0.5 fM to 100 nM. The calibration curve (Fig. 4B) displayed good linearity with the logarithm (lg) TB concentration and the liner equation was expressed as $I = 0.2712\ \lg c_{TB} + 0.7691$ ($R^2 = 0.9981$) with the detection of limit was 0.17 fM (S/N = 3). Besides, the comparison of the previously reported strategies for TB detection was shown in Table 1. Compared with recently proposed approaches of TB detection, the PEC biosensor constructed by the synergistic mechanism of quenching and sensitizing combining with bipedal DNA walker was more sensitive and possessed a lower detection limit.

3.7. Selectivity and stability of the PEC biosensor

To demonstrate the specificity of proposed PEC biosensor for TB detection, Na^+ (10 nM), Mg^{2+} (10 nM), CEA (10 nM), BSA (10 nM), PSA (10 nM) and HB (10 nM) were selected as possible interferences to compare with the PEC responses of 100 pM TB. As illustrated in Fig. S3A in the Supplementary material, we can see that the PEC responses of interferences were significantly reduced compared with TB, which similar that of the blank sample. And as shown in Fig. S3B in the Supplementary material, the PEC responses of interferences also not increased with the incremental time. These results showed an excellent selectivity of this proposed strategy for TB determination. Moreover, PEC response of this biosensor towards 20 nM TB was investigated

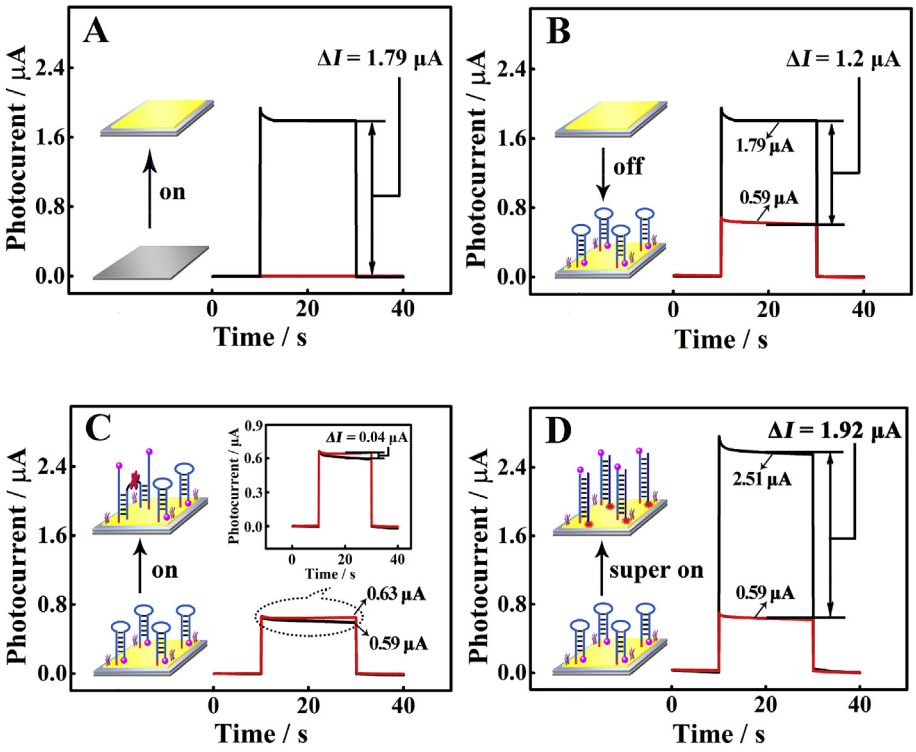

Fig. 3. The PEC response of depAu/PTCA/GCE (A) before (black line represented photocurrent response of depAu, red line represented bare electrode) and (B) after modifying with H_1-Fc (black line represented photocurrent response of depAu, red line represented H_1-Fc), and the PEC response of HT/H_1-Fc/depAu/PTCA/GCE treated with mixture of P_1, P_2 and TB (C) before (black line represented photocurrent response of H_1-Fc, red line represented P_1, P_2 and TB) and (D) after modifying with H_2-MB (The black line represented photocurrent response of H_1-Fc, the red line represented H_2-MB). (For interpretation of the references to colour in this figure legend, the reader is referred to the Web version of this article.)

under continuous off-on-off light for 8 cycles for assessing the stability. As shown in Fig. S3C in the Supplementary material, the proposed biosensor exhibited desirable stability along with approving relative standard deviation (RSD) of 0.86%.

3.8. Analysis of clinical serum samples

Furthermore, we performed the recovery experiments to demonstrate the reliability and applicability of the proposed PEC biosensor. Briefly, different concentrations of TB (0.1, 1.0, 10 and 50 nM) were separately added into 10-folddiluted human serum (obtained from the Xinqiao Hospital of Chongqing, China) and then monitored by the fabricated biosensor. Table S2 in the Supplementary material exhibited the experimental results, the recoveries for TB were from 97.7% to 105% and the relative standard deviations (RSDs) were between 1.7% and 6.6%. These results indicated that the developed biosensor had potential applications for monitoring TB in human serum.

4. Conclusions

In summary, we constructed a novel "on-off-super on" PEC biosensor for the ultrasensitive detection of TB in terms of the distance-controllable signal quenching and enhancing boosted by bipedal DNA walker. Specifically, the background signal was effectively avoided by making quencher Fc proximate to PTCA firstly. Then, the bipedal DNA walker enlarged the distance between photoactive material PTCA and quencher Fc for recovering PEC signal by opening the hairpin H_1-Fc as well as brought the sensitizer MB close to PTCA via the hybridization between hairpin H_2-MB and H_1-Fc, thereby achieving the "super on" signal. This new "on-off-super on" mode that merely adjusted the distance of quencher and sensitizer by utilizing the target-related linking probe not only avoided the background signal but also increased the detection sensitivity so as to realize the ultrasensitive detection of TB and make the detection limit down to sub-picomolar level. Moreover, the distance-controllable PEC "on-off-super on" strategy provided a promising sensing platform for ultrasensitive detection of various biomolecules in bioanalysis and disease diagnosis.

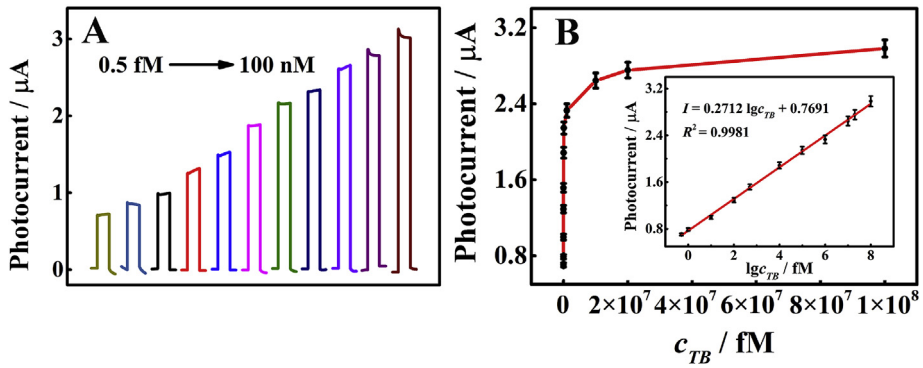

Fig. 4. (A) PEC response of this biosensor with different concentrations of TB (0.5 fM, 1.0 fM, 10 fM, 100 fM, 0.5 pM, 10 pM, 100 pM, 1.0 nM, 10 nM, 20 nM and 100 nM). (B) The calibration curve for TB detection. The standard deviation (n = 3) was represented by error bars.

Table 1
Comparison for the TB detection with other analytical methods.

Analytical method	Analytical mode	Assay time	Detection limit	Detection range	Ref.
Electrochemistry	Signal on	240 min	0.32 pM	1 pM-30 nM	Yang et al. (2017)
Electrochemistry	Signal off	50 min	1.8 pM	5 pM-5 nM	Zhu et al. (2019)
Fluorescence	Signal on	—	1 pM	0–100 nM	Lin et al. (2015)
PEC	Signal on	150 min	0.05 pM	0.1 pM-1.0 nM	Wang et al. (2018c)
PEC	Signal on	220 min	17.3 fM	87.5 fM-8.75 nM	Li et al. (2018b)
PEC	Signal on	240 min	9.6 fM	20 fM-10 pM	Li et al. (2017a)
PEC	Signal off	40 min	0.12 pM	0.5 pM-5.0 nM	Fan et al. (2016)
PEC	Signal off	—	0.02pM	0.05 pM–110 pM	(Xu et al., 2016)
PEC	Signal on-off-super on	80 min	0.17 fM	0.5 fM-100 nM	This work

Declaration of competing interest

The authors declare that they have no known competing financial interests or personal relationships that could have appeared to influence the work reported in this paper.

Acknowledgments

This work was supported by the Chongqing Research Program of Basic Research and Frontier Technology (cstc2018jcyjA0797, cstc2017jcyjAX0230), the Fundamental Research Funds for the Central Universities (XDJK2019B022, SWU117045, XDJK2018C041), and the National Natural Science Foundation (NNSF) of China (51473136, 21575116).

Appendix A. Supplementary data

Supplementary data to this article can be found online at https://doi.org/10.1016/j.bios.2019.111618.

References

Chu, Y.X., Deng, A.P., Wang, W.J., Zhu, J.J., 2019. Anal. Chem. 91, 3619–3627.
Fan, D.W., Guo, C.J., Ma, H.M., Zhao, D., Li, Y.N., Wu, D., Wei, Q., 2016. Biosens. Boelectron. 75, 116–122.
Gill, R., Zayats, M., Willner, I., 2008. Angew. Chem. Int. Ed. 47, 7602–7625.
Hou, T., Li, W., Liu, X.J., Li, F., 2015. Anal. Chem. 87, 11368–11374.
Kong, Q.K., Cui, L., Zhang, L., Wang, Y.H., Sun, J.L., Ge, S.G., Zhang, Y., Yu, J.H., 2018. Anal. Chem. 90, 11297–11304.
Lee, Y.W., Boonmongkolras, P., Son, E.J., Kim, J., Lee, S.H., Kuk, S.K., Ko, J.W., Shin, B., Park, C.B., 2018. Nat. Commun. 9, 4208.
Lei, Y.M., Wen, R.X., Zhou, J., Chai, Y.Q., Yuan, R., Zhuo, Y., 2018. Anal. Chem. 90, 6851–6858.
Lei, Y.M., Zhao, M., Wang, A., Yu, Y.Q., Chai, Y.Q., Yuan, R., Zhuo, Y., 2016. Chem. Eur J. 22, 8207–8214.
Li, C.X., Wang, H.Y., Shen, J., Tang, B., 2015. Anal. Chem. 87, 4283–4291.
Li, C.X., Lu, W.S., Zhu, M., Tang, B., 2017a. Anal. Chem. 89, 11098–11106.
Li, J., Tu, W.W., Li, H.B., Han, M., Lan, Y.Q., Dai, Z.H., Bao, J.C., 2014. Anal. Chem. 86, 1306–1312.
Li, M.J., Zheng, Y.N., Liang, W.B., Yuan, Y.L., Chai, Y.Q., Yuan, R., 2016. Chem. Commun. 52, 8138–8141.
Li, R.Y., Tu, W.W., Wang, H.S., Dai, Z.H., 2018a. Anal. Chem. 90a, 9403–9409.
Li, R.Y., Zhang, Y., Tu, W.W., Dai, Z.H., 2017b. ACS Appl. Mater. Interfaces 9, 22289–22297.
Li, Y., Chen, F.T., Luan, Z.Z., Zhang, X.R., 2018b. Biosens. Boelectron. 119, 63–69.
Lin, L.H., Liu, S.Q., Nie, Z., Chen, Y.Z., Lei, C.Y., Wang, Z., Yin, C., Hu, H.P., Huang, Y., Yao, S.Z., 2015. Anal. Chem. 87, 4552–4559.
Liu, S.S., Cao, H.J., Wang, X.Y., Tu, W.W., Dai, Z.H., 2018. Nanoscale 10, 16474–16478.
Liu, Y., Yan, K., Zhang, J.D., 2016. ACS Appl. Mater. Interfaces 8, 28255–28264.
Mei, L.P., Jiang, X.Y., Yu, X.D., Zhao, W.W., Xu, J.J., Chen, H.Y., 2018. Anal. Chem. 90, 2749–2755.
Qileng, A., Wei, J., Lu, N., Liu, W.P., Cai, Y., Chen, M.S., Lei, H.T., Liu, Y.J., 2018. Biosens. Bioelectron. 106, 219–226.
Wang, B., Mei, L.P., Ma, Y., Xu, Y.T., Ren, S.W., Cao, J.T., Liu, Y.M., Zhao, W.W., 2018a. Anal. Chem. 90, 12347–12351.
Wang, H.H., Li, M.J., Zheng, Y.N., Hu, T., Chai, Y.Q., Yuan, R., 2018b. Biosens. Bioelectron. 120, 71–76.
Wang, J., Song, M.M., Hu, C.G., Wu, K.B., 2018c. Anal. Chem. 90, 9366–9373.
Wang, K.W., Zhang, R.H., Sun, N., Li, X.P., Wang, J.N., Cao, Y., Pei, R.J., 2016. ACS Appl. Mater. Interfaces 8, 25834–25839.
Xu, F., Zhu, Y.C., Ma, Z.Y., Zhao, W.W., Xu, J.J., Chen, H.Y., 2016. Chem. Commun. 52, 3034–3037.
Yan, K., Liu, Y., Yang, Y.H., Zhang, J.D., 2015. Anal. Chem. 87, 12215–12220.
Yan, P.C., Jiang, D.S., Tian, Y.H., Xu, L., Qian, J.C., Li, H.N., Xia, J.X., Li, H.M., 2018. Biosens. Bioelectron. 111, 74–81.
Yang, X., Lv, J.J., Yang, Z.H., Yuan, R., Chai, Y.Q., 2017. Anal. Chem. 89, 11636–11640.
Yu, S.Y., Xue, T.Y., Zhu, L.B., Fan, G.C., Han, D.M., Wang, C.S., Zhao, W.W., 2019. Biosens. Bioelectron. 136, 128–131.
Zhang, G.Y., Shan, D., Dong, H.F., Cosnier, S., Al-Ghanim, K.A., Ahmad, Z., Mahboob, S., Zhang, X.J., 2018a. Anal. Chem. 90, 12284–12291.
Zhang, N., Shi, X.M., Guo, H.Q., Zhao, X.Z., Zhao, W.W., Xu, J.J., Chen, H.Y., 2018b. Anal. Chem. 90, 11892–11898.
Zhao, W.W., Xu, J.J., Chen, H.Y., 2015. Chem. Soc. Rev. 44, 729–741.
Zhao, W.W., Xu, J.J., Chen, H.Y., 2014. Chem. Rev. 114, 7421–7441.
Zeng, R.J., Luo, Z.B., Su, L.S., Zhang, L.J., Tang, D.P., Niessner, R., Knopp, D., 2019a. Anal. Chem. 91, 2447–2454.
Zeng, R.J., Zhang, L.J., Su, L.S., Luo, Z.B., Zhou, Q., Tang, D.P., 2019b. Biosens. Bioelectron. 133, 100–106.
Zhu, C.H., Zhu, W.Y., Xu, L., Zhou, X.M., 2019. Anal. Chim. Acta 1047, 21–29.